

## Analysis of Electron Internal Transport Barriers in JET low and reversed shear discharges

G.M.D. Hogeweij<sup>1</sup>, H.J. de Blank<sup>1</sup>, C. Bourdelle<sup>2</sup>, N. Hawkes<sup>3</sup>, F. Imbeaux<sup>2</sup>,  
N. Kirneva<sup>4</sup> and JET-EFDA contributors \*

<sup>1</sup> FOM Institute for Plasma Physics Rijnhuizen, Association EURATOM-FOM, Trilateral Euregio Cluster, P.O.Box 1207, Nieuwegein, The Netherlands, [www.rijnh.nl](http://www.rijnh.nl)

<sup>2</sup> Association EURATOM-CEA, CEA/DSM/DRFC, CEA Cadarache, France

<sup>3</sup> Euratom/UKAEA Fusion Association, Culham Science Centre, Abingdon, UK

<sup>4</sup> Nuclear Fusion Institute, RRC Kurchatov Institute, Moscow, Russia

**1. Introduction.** The study of electron thermal transport and electron Internal Transport Barriers (eITBs) in regimes with dominant electron heating is of great importance for ITER. Single JET pulses with eITB were studied in [1,2]. In this paper for the first time a consistent study of 15 predominantly electron heated JET pulses with and without eITB is presented, covering the full range of safety factor ( $q$ ) profiles, from strongly reversed shear ( $s$ ) via low shear to standard positive shear. The difference in  $q$  profiles is mainly brought about by the use of various Lower Hybrid (LH) power levels.

The presence of eITBs in the experiments is analyzed in two ways. First, local reduction of electron thermal diffusion is searched for by means of local power balance analysis, performed with the CRONOS code [3]. CRONOS is also used to calculate the current driven by LH, which is an essential ingredient to calculate  $q$ . For many pulses no or very limited Motional Stark Effect data (from which  $q$  is derived) are present; when MSE data are available, they will be compared with the CRONOS calculations.

Second, the so-called  $\rho_T^*$  ITB analysis [4] is used; here an eITB manifests itself as a local enhancement of the dimensionless parameter  $\rho_{T_e}^* = \rho_s/L_{T_e}$ , where  $\rho_s$  is the ion Larmor radius at sound speed and  $L_{T_e}$  the local  $T_e$  gradient scale length.

Linear microturbulence analysis with KineZero [5] is performed for these pulses to assess linear growth rates ( $\gamma_{lin}$ ) in both the ITG-TEM and ETG range of wavelengths. This paper addresses the following questions:

- Dependence of sustainment and quality of eITB on  $s$ .
- Relation between experimentally observed eITB and stabilization of instabilities.
- Parametric dependence of  $\gamma_{lin}$  on plasma parameters, in particular  $s$  and the  $T_e$  inverse gradient length ( $A_{T_e}$ ).

**2. eITB analysis and relation with magnetic shear.** As typical for the dataset, the JET pulses 62796/97 are compared, which had the same scenario apart from LH power, see Fig.1. The  $\rho_T^*$  eITB analysis, plotted in Fig.2, shows a clear difference between the two pulses: whereas 62797 loses the eITB after the preheat phase, 62796 sustains the eITB in the current flat top phase, albeit at a smaller radius than in the preheat phase.

Fig.3 shows the profiles of  $\chi_e$ ,  $q$ ,  $s$  (as calculated by CRONOS),  $q$  from MSE, and  $\rho_{T_e}^*$  for these two pulses during the steady state phase at 8 s. The  $q$  profiles from MSE are in fair agreement with  $q$  from CRONOS: for 62797 both are monotonic; for 62796 both have a minimum at nearly the same position. At this time the eITB is only present in 62796, i.e. in the pulse with reversed shear, and located just inside  $q_{min}$ . Note the good match of maximum  $\rho_{T_e}^*$  and minimum  $\chi_e$  for pulse 62796. In the preheat phase (not shown here) both pulses have an eITB and reversed shear.

---

\* See the Appendix of J.Pamela et al., *Fusion Energy 2004 (Proc. 20th Int. Conf. Vilamoura, 2004)* IAEA, Vienna (2004)

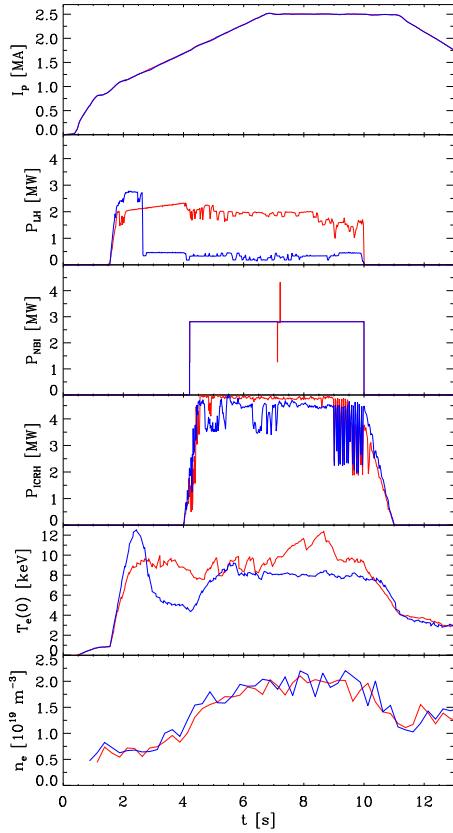


Figure 1: Scenario of JET pulses 62796 and 62797: the panels show the time evolution of  $I_p$ ,  $P_{LH}$ ,  $P_{NBI}$ ,  $P_{ICRH}$ ,  $T_e(0)$ , and  $n_e$ .

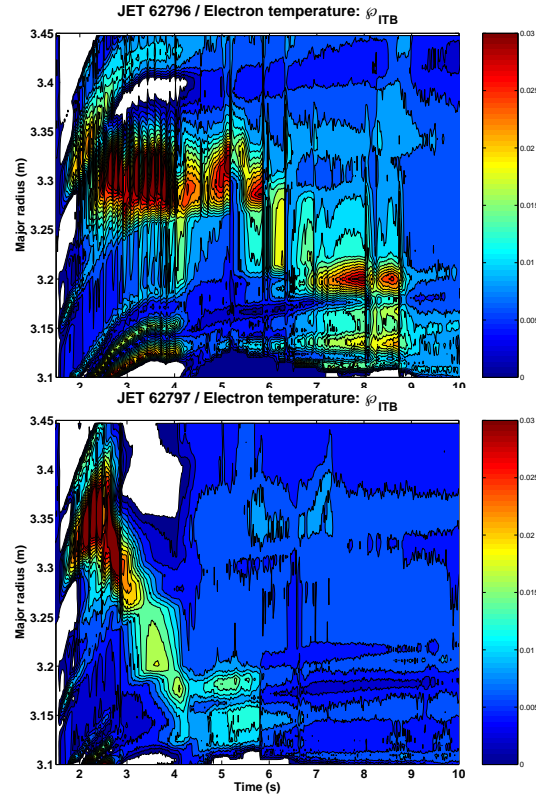


Figure 2:  $\rho_{T_e}^*$  electron ITB analysis for the two pulses of Fig.1, showing a striking difference in evolution. The colours indicate the value of  $\rho_{T_e}^*$ ; a value of 0.014 is considered as ITB margin.

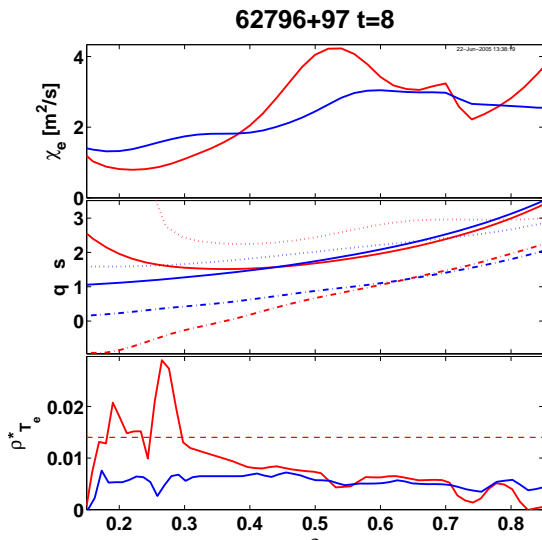


Figure 3: Profiles for 62796 and 62797 at 8 s. Upper panel:  $\chi_e$ ; middle panel:  $q$  (full) and  $s$  (dashed lines) as calculated by CRONOS, and  $q$  from MSE (dotted lines); lower panel:  $\rho_{T_e}^*$ .

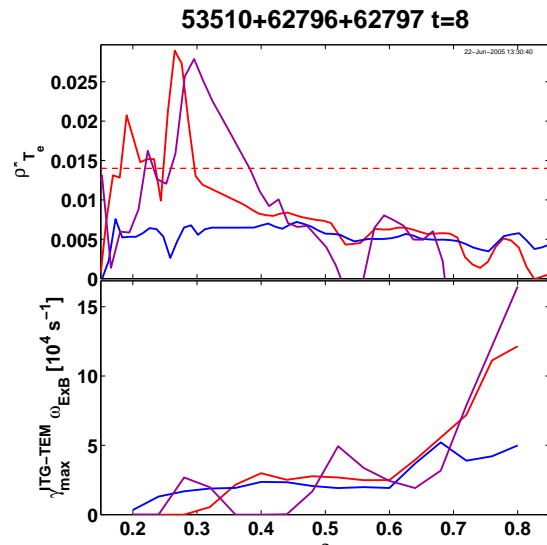


Figure 4: Profiles of  $\rho_{T_e}^*$  (upper panel) and  $\gamma_{\max}^{\text{ITG-TEM}}$  (lower panel) for 53510, 62796 and 62797 at 8 s.

**3. Link between eITB observation and suppression of instabilities.** In most cases suppression of the ITG-TEM branch of microturbulence, as calculated with KineZero, corresponds fairly well with the presence of an eITB. Fig.4 compares  $\rho_{T_e}^*$  with  $\gamma_{\max}^{\text{ITG-TEM}}$  for the two pulses analyzed in the previous section, plus pulse 53510, which will be analyzed further on. The presence/absence of an eITB inside  $\rho = 0.3$  for 62796/97 is reflected in absence/presence of turbulence in the same region. For pulse 53510, the area of suppressed instabilities lies at somewhat larger radius than the eITB. The ETG branch of turbulence (not shown here) generally only plays a role in the outer part of the plasma ( $\rho > 0.7$ ).

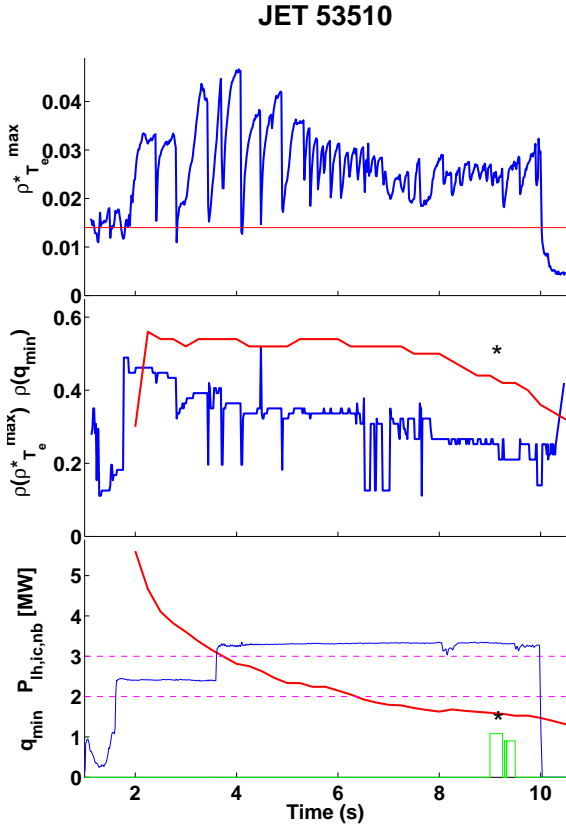


Figure 5: Time traces for pulse 53510. Upper:  $\rho_{T_e}^{* \max}$  and ITB criterion; middle:  $\rho(\rho_{T_e}^{* \max})$  and  $\rho(q_{\min})$  (from CRONOS); lower:  $q_{\min}$  (from CRONOS),  $P_{\text{LH}}$  and  $P_{\text{NBI}}$ . In this pulse there was only a short NBI blip, resulting in just 1 MSE data point; the asterisks in the 2nd and 3rd panel indicate  $\rho(q_{\min})$  and  $q_{\min}$  from MSE.

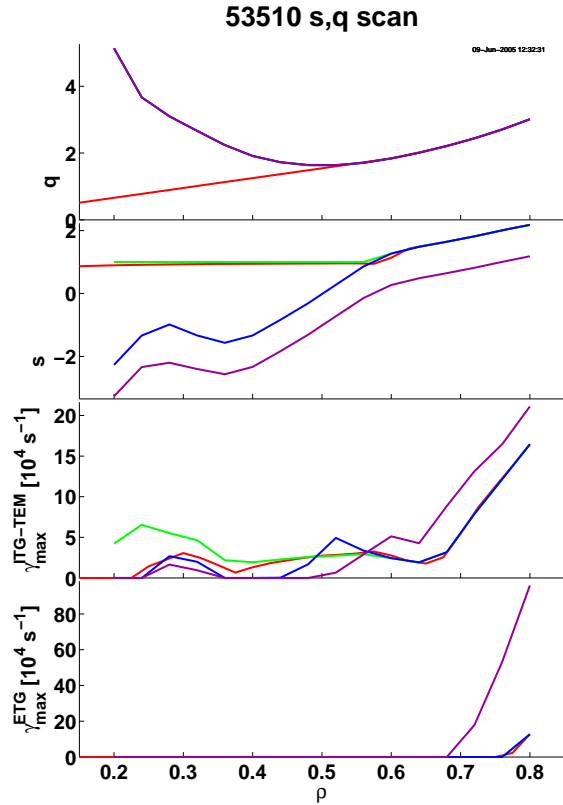


Figure 6: KineZero microturbulence calculations for pulse 53510 at  $t = 8$  s (blue), and for cases with artificially decreased  $s$  (violet), and increased  $s$  (green with unchanged  $q$ ; red with consistently changed  $q$ ).

**4. Link between  $s$  and suppression of instabilities.** This is tested starting from JET pulse 53510, which had a well-established eITB. Fig.5 shows the time evolution of the maximum value of  $\rho_{T_e}^*$  ( $\rho_{T_e}^{* \max}$ ), its position  $\rho(\rho_{T_e}^{* \max})$ , the position of  $q_{\min}$ , as calculated by CRONOS,  $q_{\min}$ , and the input power levels. The eITB resides at  $\simeq 10\%$  smaller radius than  $q_{\min}$ . The single MSE data point available is also plotted (asterisks), and shows satisfactory agreement with the CRONOS result.

Then Fig.6 shows the KineZero calculations of  $\gamma_{\max}^{\text{ITG-TEM}}$  and  $\gamma_{\max}^{\text{ETG}}$ . KineZero was run for the profiles as calculated by CRONOS (blue) and for cases with artificially de-

creased (violet) and increased  $s$  (green, red). It is clearly seen that the level of ITG-TEM turbulence in the eITB region ( $\rho \sim 0.2 - 0.4$ ) strongly depends on  $s$ : the turbulence is strongly enhanced for positive  $s$ , and is further suppressed for more negative  $s$ .

**5. KineZero study of  $A_{T_e}$  dependence of turbulence.** The analysis of the dependence of microturbulence on inverse gradient length ( $A_{T_e}$ ) is done starting again from pulse 53510.  $A_{T_e}$  is doubled and halved for both the experimental  $s$  profile, and for an artificial monotonic  $s$  profile;  $T_e$  itself is left unchanged, so this is really a test of the effect of local steepening of  $\nabla T_e$ . The results are shown in Fig.7. In the eITB region the ITG-TEM turbulence is insensitive for  $A_{T_e}$ ; in contrast, for positive  $s$ , a strong increase of microturbulence with  $A_{T_e}$  is seen.

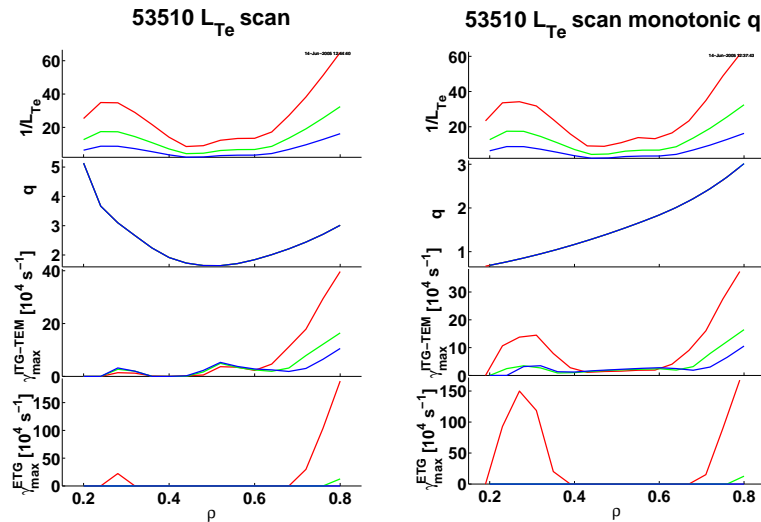


Figure 7: *KineZero study of  $A_{T_e}$  dependence of turbulence, based on pulse 53510, for (left) experimental  $q$  and (right) monotonic  $q$ . 1st panel:  $A_{T_e}$  2nd:  $q$ ; 3rd:  $\gamma_{\max}^{\text{ITG-TEM}}$ ; 4th:  $\gamma_{\max}^{\text{ETG}}$ . Shown are results for *experimental, doubled and halved  $A_{T_e}$ .**

**6. Conclusions.** In the type of pulses studied, i.e. with dominant e heating and low momentum input, eITB strength is mainly determined by  $s$ . Considering the whole dataset (now shown here), there appears to be no sharp transition between plasmas with and without eITB.

MSE data availability for the present dataset is scarce. When available, the MSE data are in good agreement with the CRONOS calculations; this gives us confidence that we can rely on the CRONOS results also for cases where MSE is not available.

The experimental signatures of eITBs correspond well with the findings of microturbulence calculations. Moreover, these calculations confirm the central role of  $s$ . This role of negative  $s$  in ITB formation corroborates results of turbulent transport modeling [6]. With negative shear, increasing inverse gradient length does not enhance the turbulence - a true sign of an ITB.

**Acknowledgements.** This work, supported by the European Communities under the contract of Association between EURATOM/FOM, was carried out within the framework of the European Fusion Programme with financial support from NWO. The views and opinions expressed herein do not necessarily reflect those of the European Commission.

## References

- [1] Hogewij G.M.D. et al, *Plasma Phys. Contr. Fusion* **42** (2002) 1155
- [2] Kirneva N. et al, Controlled Fusion and Plasma Physics (Proc. 31th Eur. Conf., London, UK, 2004), CD-ROM file P-1.152
- [3] Basiuk V. et al, *Nucl. Fusion* **43** (2003) 822
- [4] Tresset G. et al, *Nucl. Fusion* **42** (2002) 520
- [5] Baranov Yu. et al, *Plasma Phys. Contr. Fusion* **46** (2004) 1181
- [6] Bourdelle C. et al, *Nucl. Fusion* **42** (2002) 892